J Mater Sci (2008) 43:6468–6472
DOI 10.1007/s10853-008-2982-6

Three-dimensional (3D) modeling of the thermoelastic behavior of woven glass fiber-reinforced resin matrix composites

X. Deng · N. Chawla

Received: 30 May 2008 / Accepted: 2 September 2008 / Published online: 17 September 2008

Abstract The thermoelastic behavior of glass fiber-reinforced resin matrix composites is very important in several applications such as electronic packaging. Simulation of the composite behavior is complicated because of the complex nature of woven fiber architecture. In this study, we have conducted a numerical simulation of elastic and thermal expansion behavior of woven glass fiber-reinforced resin matrix composite. The simulations were compared to experimental data, showing excellent agreement with elastic properties and fairly good results for the thermal expansion coefficient of the composite.

Introduction

Glass fiber-reinforced resin matrix composites are used in a variety of applications. In electronic packaging they are used due to the lightweight, electronic insulation, and thermo-mechanical stability [1]. The electronic packaging industry is undergoing significant changes due to the advent of environmental-benign solders with higher melting point than Pb–Sn solders [2–5]. The printed circuit board (PCB), which is typically made of a glass fiber-reinforced resin matrix composite, will have to withstand higher reflow temperatures. Thus, it is extremely important to understand the thermoelastic behavior of the PCB, which is directly related to the reliability of the electronic package.

Experimental and numerical investigations have been made on the thermal and mechanical stability of PCBs [6–14]. Most of the research has focused on the solder–PCB interface rather than the PCB itself. Furthermore, the PCB is usually considered as a homogeneous material. While the micromechanics of fiber-reinforced polymer matrix composites has been the subject of many studies [15–22], it has not been as widely employed to study thermoelastic behavior. A microstructure-based approach is necessary to capture the important features of the woven fiber fabric in the resin matrix.

In this study, we have used finite-element simulations to model and predict the thermal and elastic properties of a glass fiber-reinforced resin matrix composite. The microstructure of the fibrous reinforcement, and in particular, the geometry of glass fiber bundle, was explicitly considered in the simulations. Both the Young's modulus and the coefficient of thermal expansion were investigated in the temperature range of 21 to 150 °C. The predicted values were in good agreement with experimental results obtained by Isola Laminates.

Finite-element method simulation procedures

In this study, finite-element method (FEM) (Abaqus, Simulia, RI) was employed to simulate the thermoelastic behavior of the composites. The FEM model was constructed based on the microstructure of woven glass fiber-reinforced resin matrix PMC as shown in Fig. 1a. The glass fiber bundle, consisting of many fibers, is embedded in a resin matrix. Inside the glass bundle there is a very small fraction of resin. The volume fraction of glass with respect

X. Deng · N. Chawla (✉)
School of Materials, Fulton School of Engineering,
Arizona State University, Tempe, AZ 85287-8706, USA
e-mail: nchawla@asu.edu

Present Address:
X. Deng
Kennametal, Rogers, AR, USA

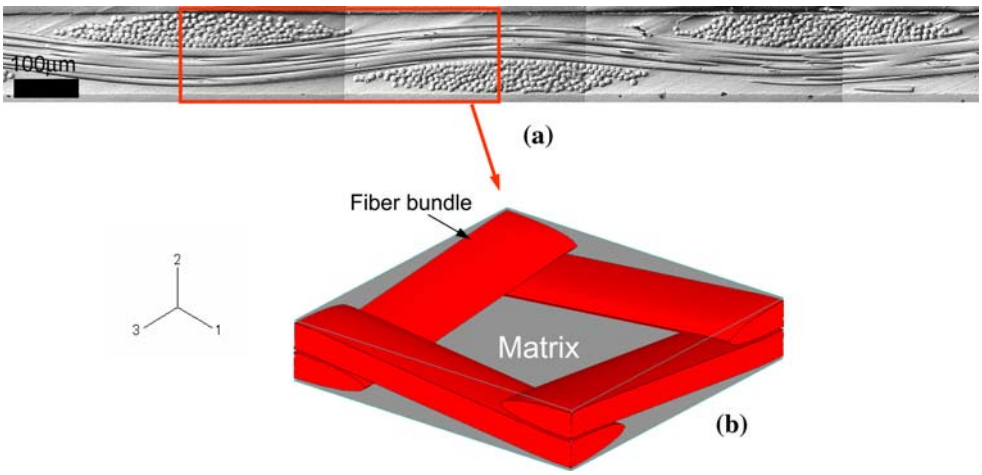

Fig. 1 (**a**) Microstructure of glass fiber-reinforced resin matrix PMC. The cross section of glass fiber bundle is elliptical. Glass fiber bundle contains about 75 vol.% glass fiber and the glass fiber has about 35 vol.% with respect to the whole composite. (**b**) Unit cell of PMC for FEM, where the glass fiber bundle was simplified into a single fiber. The fiber volume fraction is 35%, which is identical to the actual PMC

to the whole composite is ~35% and the volume fraction of glass fiber inside the glass bundle is around 75%. These were measured by image analysis of several sections and also correlated well with data provided by the manufacturer (Isola Laminates, Chandler, AZ). The fiber bundles can be modeled in two ways: (a) simplifying the bundle to be a solid block of glass, and (b) assuming the bundle to be a composite consisting of 75 vol.% glass fiber. In this study, models with both "types" of bundles were employed and compared.

A unit cell of the woven fiber fabric reinforced with resin was constructed based on the microstructure of the actual composite (Fig. 1b). In this model, the glass bundle is modeled as a solid material, either pure glass or a composite of glass and resin, with elliptical shape. Figure 2 shows details of the finite-element mesh. The mesh type used was a Quadratic 3D Stress Tetrahedron to conform to the complex shape of the fiber bundle. Table 1 shows the thermoelastic properties used for both glass fiber and resin matrix. These were provided by the manufacturer.

Table 1 Thermoelastic properties of glass fiber and resin matrix

	Young's modulus (GPa)	Poisson's ratio	CTE (10^{-6}/°C)
Resin matrix	3.8	0.35	59.0
Glass fiber	73	0.22	5.0

Figure 3 shows the boundary conditions for elastic deformation and calculation of the Young's modulus in the three orthogonal directions. The displacement of the surface normal to the loading axis was fixed. Tensile loading was applied in directions 1–3, and Young's modulus calculated. For the thermal simulation, the temperature was varied from 21 to 150 °C. Figure 4 shows the boundary conditions for thermal simulation. The displacement of three surfaces was constrained, and the CTE in each of the three directions was calculated.

The modeling results were compared with experimental data. The Young's modulus of the composites in all three directions was measured by uniaxial tensile testing of

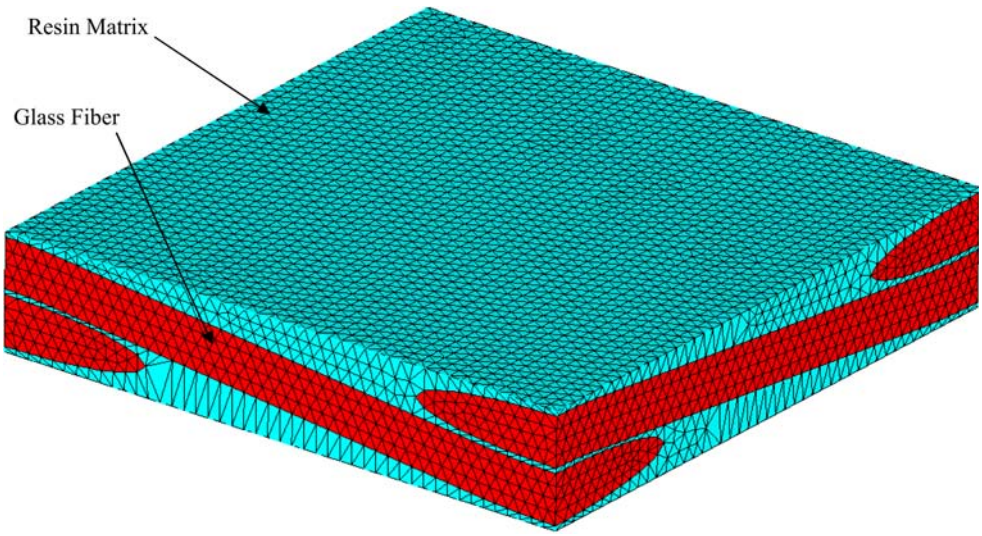

Fig. 2 Mesh details for unit cell used in the simulations. The mesh type is a Quadratic 3-D Stress Tetrahedrom

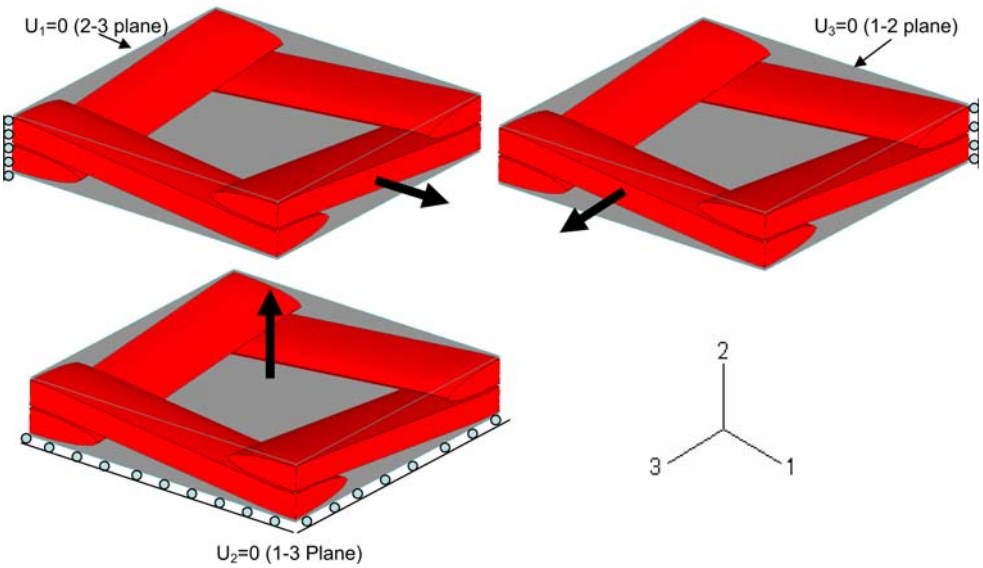

Fig. 3 Boundary conditions for simulation of elastic deformation. Tensile load was applied in directions 1–3 to investigate the Young's modulus in these directions

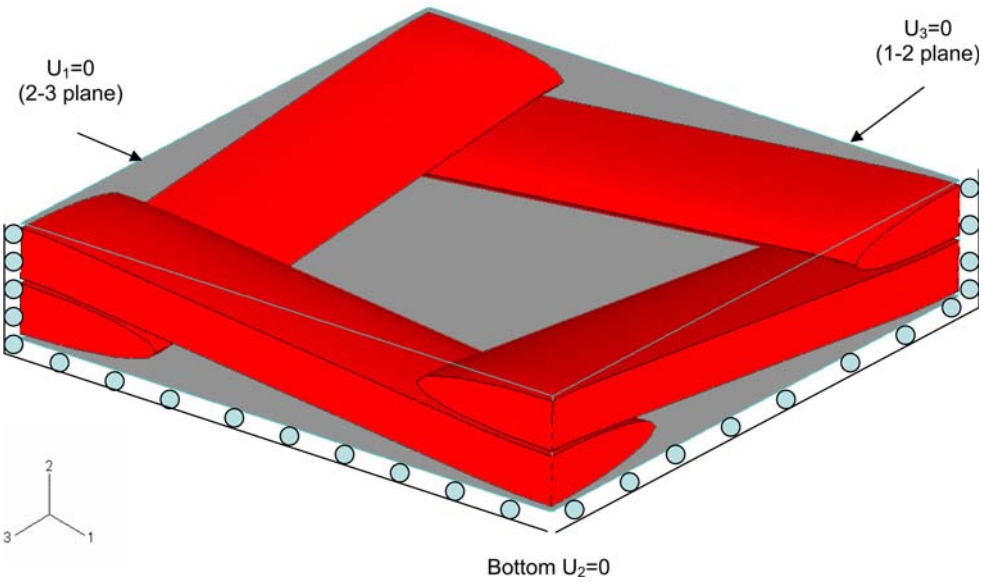

Fig. 4 Boundary conditions used for simulation of thermal expansion

dog-bone shaped specimens on a servohydraulic machine (the direction of interest was machined parallel to the loading axis). Strain was measured with a clip-on extensometer. The coefficient of thermal expansion was measured with a linear thermal analysis instrument that was employed to obtain the thermal displacement of the specimens. A glass pushrod was used for the measurement of the thermal expansion displacement of the sample. The thermal expansion of the sensing glass pushrod was measured without the sample being present to subtract the contribution from expansion of the rod itself. The expansion of the pushrod was negligible ($\sim$0.5 μm from 25 to 150 °C), relative to that of the CTE of the composites samples and was therefore ignored. The temperature was continuously cycled between 25 and 120 °C to obtain the CTE.

Results and discussion

The results from purely elastic loading of the woven fiber fabric-reinforced resin matrix composite are shown in Fig. 5a. Very good agreement is obtained with the experimental data. Direction 1 has a higher fraction of fibers along the direction of loading, so it has the highest modulus. Next is direction 3 which is also in-plane, but has a lower volume fraction of fibers parallel to its direction. Finally, direction 2 is the transverse direction, and, thus, has the lowest modulus. The deformation of the fabric is quite different from a conventional fiber-reinforced composite because the fibers undulate over and under other fiber bundles. Stress concentrations are often observed at the "cross-over" points between fiber bundles [23, 24]

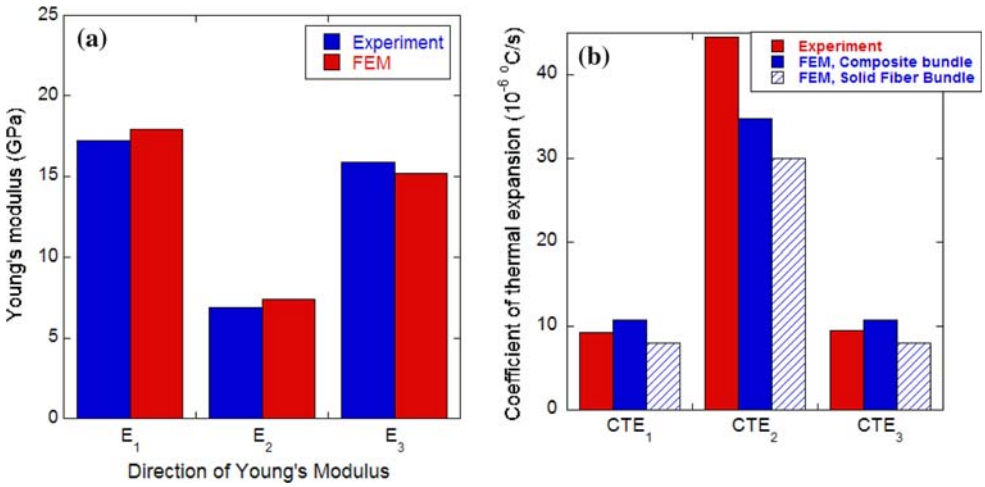

Fig. 5 Comparison of FEM predictions with experiment: (**a**) Young's modulus and (**b**) coefficient of thermal expansion. Good agreement is observed between experiment and model

during tensile loading. The straightening process results in localized fracture at the cross-over points.

Modeling of the thermal behavior, as mentioned above, was carried out by assuming a pure solid glass bundle and by assuming a composite bundle. The composite glass fiber bundle can be considered as a unidirectional continuous fiber-reinforced composite, so the elastic and thermal properties should be anisotropic. In the longitudinal direction (fiber longitudinal direction), the Young's modulus, the fibers, and matrix are in an isostrain condition, so the longitudinal modulus of the composite, E_L, is given by [25]:

$$E_L = E_f V_f + E_m V_m, \quad (1)$$

where E_f and E_m are the Young's modulus of fiber and matrix, respectively, and V_f and V_m are the volume fraction of fiber and matrix, respectively. In the transverse direction (normal to the fiber longitudinal direction), the Young's modulus can be calculated using the isostress model [25]:

$$E_t = \frac{1}{V_f/E_f + V_m/E_m}. \quad (2)$$

Similarly the directionality in thermal expansion can be calculated with Schapery's analytical model [26]. The longitudinal thermal expansion, α_L, is given by:

$$\alpha_L = \frac{\alpha_f E_f V_f + \alpha_m E_m V_m}{E_f V_f + E_m V_m}, \quad (2)$$

where α_f and α_m are the CTE of fiber and matrix, respectively. The CTE in the transverse direction, also calculated by Schapery's model, is given by [26]:

$$\alpha_t = (1+\nu_m)\alpha_m V_m + (1+\nu_f)\alpha_f V_f - \alpha_L(\nu_f V_f + \nu_m V_m). \quad (4)$$

Using the above equations, the anisotropic elastic and thermal properties of the "composite bundle" are given in Table 2. These composite bundles are, of course, surrounded by pure resin matrix.

Table 2 Thermoelastic properties of composite fiber bundle for FEM input

Longitudinal			Transverse		
E (GPa)	ν	α (10^{-6}/°C)	E (GPa)	ν	α (10^{-6}/°C)
55.7	0.22	5.96	13.1	0.33	23

Figure 5b shows the coefficient of thermal expansion along the three directions. The CTE along the 2-axis is highest due to the least constraint from the fibers. The in-plane CTE is significantly reduced along the longitudinal direction of the fibers. FEM predicts the in-plane CTE values relatively well. Along the 2-axis, however, the FEM predictions underpredict the experiment. The use of a "composite bundle" as opposed to a solid glass fiber bundle does improve the prediction. Figure 6 shows the von Mises stress contour plot during the heating of the composite. Note that the longitudinal fibers develop a stress concentration due to severe expansion in the two directions. This stress is highest in the center of the longitudinal fibers, away from the constraint imposed by the overlapping fiber bundle.

Summary

A numerical analysis of the Young's modulus and coefficient of thermal expansion of woven glass fiber-reinforced resin matrix composites was conducted. The complex geometry of the woven structure was captured in a unit cell model. The fiber bundles were modeled as pure glass fiber bundles and as anisotropic composite bundles. The values from finite-element analysis correlated well with those from experiments.

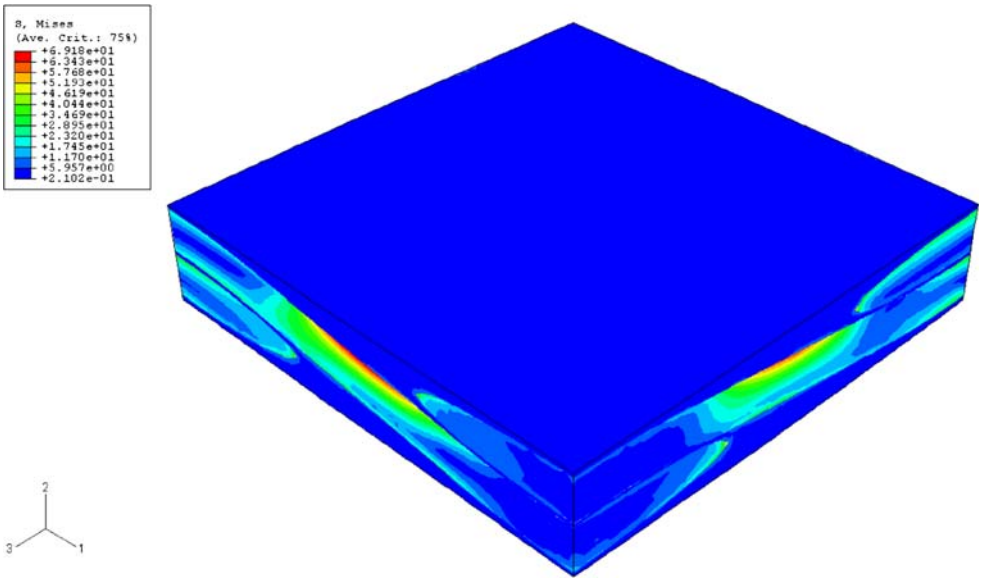

Fig. 6 Von Mises stress contour plots showing stress concentration in longitudinal fiber bundle, due to severe thermal expansion in the two directions, for a temperature change of about 130 °C

Acknowledgements The authors acknowledge the financial support for this work from Isola Laminates Inc. We thank Mr. Tarun Amla for providing the experimental data for Young's modulus and coefficient of thermal expansion.

References

1. Kutz M (ed) (2002) Handbook of materials selection. Wiley, New York
2. Glazer JJ (1994) J Electron Mater 23(8):693. doi:10.1007/BF02651361
3. Wood EP, Nimmo KL (1994) J Electron Mater 23:709. doi:10.1007/BF02651363
4. Abtew M, Selvardery G (2000) Mater Sci Eng Rep 27:95. doi:10.1016/S0927-796X(00)00010-3
5. Deng X, Piotrowski G, Williams JJ, Chawla N (2003) J Electron Mater 32:1403. doi:10.1007/s11664-003-0108-0
6. Wu CML, Lai JKL, Wu YL (1998) Finite Elem Anal Des 30:19. doi:10.1016/S0168-874X(98)00028-6
7. Yamada SE (1987) Eng Fract Mech 27:315. doi:10.1016/0013-7944(87)90149-4
8. Rice JR (1988) J Appl Mech Trans ASME 55:98
9. Xie DJ, Wang ZP (1998) Finite Elem Anal Des 30:31. doi:10.1016/S0168-874X(98)00032-8
10. Darveaux R, Banerji K, Mawer A, Dody G (1995) In: Lau JH (ed) Ball grid array technology. McGraw-Hill, New York, p 379
11. Solomon HD (1994) In: Fear DR, Burchett SN, Morgan HS, Lau JH (eds) The mechanics of solder alloy interconnects. Van Norstrand Reinhold, New York, p 199
12. Yang QJ, Shi XQ, Wang ZP, Shi ZF (2003) Finite Elem Anal Des 39:819. doi:10.1016/S0168-874X(02)00134-8
13. Lau JH, Pao YH (1997) Solder joint reliability of BGA, CSP, flip chip, and fine pitch smt assemblies. McGraw-Hill, New York
14. Shi XQ, Zhou W, Pang HLJ, Wang ZP (1999) J Electron Packaging 121(3):179. doi:10.1115/1.2792681
15. Tabiei A, Ivanov I (2004) Int J Non-linear Mech 39:175. doi:10.1016/S0020-7462(02)00067-7
16. Ishikawa T, Chou TW (1982) J Compos Mater 16:2. doi:10.1177/002199838201600101
17. Hahn HT, Tsai SW (1973) J Compos Mater 7:102
18. Naik RA (1995) J Compos Mater 29:2334
19. Ivanov I, Tabiei A (2001) Compos Struct 54(4):489. doi:10.1016/S0263-8223(01)00121-0
20. Seifert OE, Schumacher SC, Hansen AC (2003) Compos Part B 34:571. doi:10.1016/S1359-8368(03)00078-7
21. Zako M, Uetsuji Y, Kurashiki T (2003) Compos Sci Technol 63:507. doi:10.1016/S0266-3538(02)00211-7
22. Ellyin F, Xia Z, Chen Y (2002) Compos Part A 33:399. doi:10.1016/S1359-835X(01)00112-9
23. Chawla N, Tur YK, Holmes JW, Barber JR, Szweda A (1998) J Am Ceram Soc 81:1221
24. Shuler SF, Holmes JW, Wu X, Roach D (1993) J Am Ceram Soc 76:2327. doi:10.1111/j.1151-2916.1993.tb07772.x
25. Chawla N, Chawla KK (2006) Metal matrix composites. Springer, New York
26. Schapery RA (1968) J Compos Mater 2:380. doi:10.1177/002199836800200308